ELSEVIER

Journal of Power Sources 108 (2002) 185–191

JOURNAL OF POWER SOURCES

www.elsevier.com/locate/jpowsour

Influence of pore-size distribution of diffusion layer on mass-transport problems of proton exchange membrane fuel cells

Chang Sun Kong*, Do-Young Kim, Han-Kyu Lee, Yong-Gun Shul, Tae-Hee Lee

Department of Chemical Engineering, Yonsei University, 134 Shinchon-Dong, Sudaemoon-Ku, 120-749, Seoul, South Korea

Received 6 August 2001; accepted 2 January 2002

Abstract

The influence of pore-size distribution of the diffusion layer on mass-transport problems of proton exchange membrane fuel cells (PEMFCs) is investigated using electrodes with hydrophobic diffusion layers for which the pore-size distribution is designed by pore-former and heat treatment. It is confirmed that the pore-size distribution of the diffusion layer is a more critical parameter for mass-transport processes within the electrode and for cell performance characteristics than the total porosity itself. Data obtained from mercury intrusion porosimetry, single-cell performance tests and ac impedance analyses indicate that the performance loss due to mass-transport limitations can be reduced by enlarging the macropore volume in the diffusion layer. The water flooding problem is discussed in terms of condensation phenomena which are dependent on pore-size.

Keywords: Mass-transport; Water flooding; Diffusion layer; Pore-size distribution; Proton exchange membrane fuel cell

1. Introduction

To establish the future of the proton exchange membrane fuel cell (PEMFC) as an alternative power source, it must have high power and minimal volume. Hence, in order to ensure, without spatial concession, high power from a commercial-scale system, it is predicted that cell operation at a higher current condition per unit electrode area will be necessary. Mass-transport problems, which contribute to performance loss especially at the high current densities, are therefore becoming an important issue.

Mass-transport problems in the PEMFCs can be classified into three categories: (i) water flooding, i.e. liquid water entrapped inside the electrodes or flow channels interrupts the flux of reactant/product gases; (ii) dilution of oxidant concentration due to the use of air instead of pure oxygen; (iii) depletion of reactants along the flow channel, which results in non-uniform current distribution over the whole electrode area, and is particularly severe in a large-scale fuel cell. First, water flooding often acts as the main cause of serious performance drop at high current densities. Once liquid water fills up the pores in the electrode, this liquid barrier produces a dead reaction zone and reduces the effective electrode area. Second, even though it is essential, from practical aspects, to develop air-operated PEMFCs, the power density produced in air-fed regime is relatively low compared with that of oxygen operation. This is because the decreased partial pressure of oxygen slows down the oxygen reduction reaction and rapidly degrades cell performance. Furthermore, pressurization of the cathode side for circumventing this problem deteriorates the energy efficiency of the total system operation. Finally, inefficient flow field design can lead to a decrease of reactant utilization and active electrode area by which fuel and oxidant gas are supplied into the electrode with locally different concentration distributions. In the present study, the mass-transport-limiting condition refers to the internal situation of the fuel cell during operation in which the transport rate of reactants to the catalytic sites is the rate-determining step of the overall reaction process. Therefore, the effect of membrane dehydration caused by poor humidification is not considered in above consideration, even though it reduces the proton conductivity of the electrolyte and affects the rate of the electrochemical reaction.

In order to minimize the performance loss due to mass-transport limitation, it is important that every mass-transport problem mentioned above is taken into account along with optimization of the cell operating parameters, the configuration of the gas flow field, and the characteristics of the

* Corresponding author. Tel.: +82-2-312-6507; fax: +82-2-312-6401.
E-mail address: energy72@korea.com (C.S. Kong).

0378-7753/02/$ – see front matter
PII: S0378-7753(02)00028-9

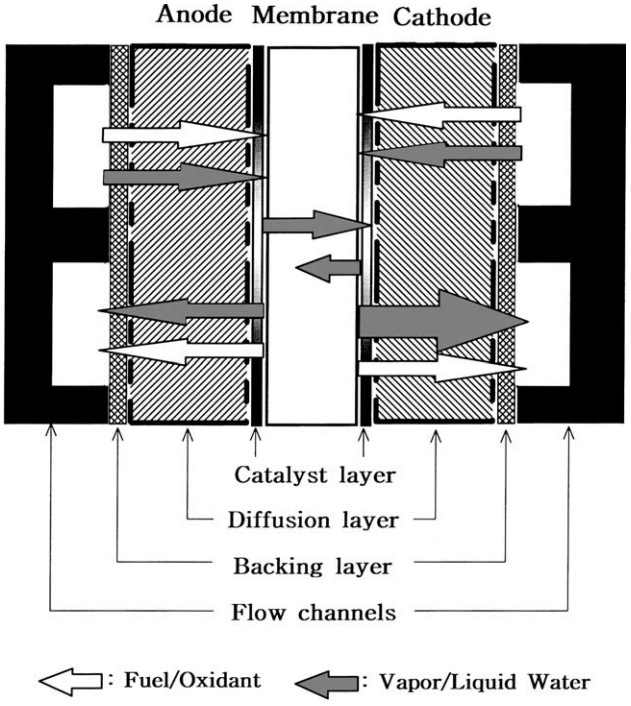

Fig. 1. Schematic diagram of configuration and mass-transport mechanism within membrane-electrode assembly.

membrane-electrode assemblies (MEAs). The anode water removal technique developed by Voss et al. [1] and the interdigitated (dead-ended) flow field design devised by Nguyen and co-workers [2,3] are two different approaches proposed for water management in PEMFCs.

An equally important factor for efficient mass-transport management is to tailor the electrode structure through the control of material properties, composition, preparation methods, etc. To design the electrode structure for PEMFCs, it should be recognized that the electrode is a field where multi-component and multi-phase flows are taking place. As illustrated in Fig. 1, vapor or liquid phase water is, along with fuel and oxidant gas, entering and exiting through the diffusion path in the electrode. Electrodes used for PEMFCs have, in general, two- or three-layered structures that can be divided into two parts, viz. catalytic and non-catalytic. The catalytic part, i.e. the catalyst layer, is formed by depositing a mixture of carbon-supported platinum catalyst and solubilized electrolyte on one side of the non-catalytic part; electrons, protons and water molecules are produced in this region. By contrast, a hydrophobic carbon layer interposed between the catalyst layer and the backing substrate, i.e. the diffusion layer, though it has no catalytic reaction sites, is known to play a key role in providing good access of reactants towards catalytic sites and effective removal of product water from the electrode [4–12]. Many studies [4,6,9–12] have demonstrated the importance of morphology of diffusion layer. Nevertheless, there have been very different interpretations and experimental results for the relation between the pore structure of diffusion layer and the cell performance.

In the present work, an examination is made of the influence of the pore-size distribution of the diffusion layer on the cell performance characteristics of PEMFCs. For this, a pore-forming step with a pore-former is included in the fabrication process of the diffusion layer, and then cell performance is measured for varying amounts of pore-former. Pore-formers have long been used by many research groups in order to modify the electrode structure. In recent years, Fischer et al. [13] and Passalacqua et al. [14] reported independently details of the improvement of air-operated cell performance by introducing pore-former to the catalyst layer. In the former studies [13], no improvement in performance was obtained when using oxygen oxidant. This may be due to the fact that the effect of water flooding at the cathode was minimized by using dry oxidant gas. Therefore, the performance enhancement of the air-fed cell leads to the conclusion that increased porosity of the catalyst layer by the pore-former has an effect on mass-transport limitation due to nitrogen gas in air. The present studies are focused mainly on oxygen operation with external humidification in order to consider the water flooding problem within the electrode. Also, the effects on air-fed cell performance are presented.

2. Experimental

2.1. Preparation of membrane-electrode assembly

Electrodes were prepared by the following three-step process, which included several pretreatment procedures. The first step was to deposit a diffusion layer on the carbon cloth substrate. Carbon powder (Vulcan XC-72, Cabot Co.), PTFE (60 wt.%, Aldrich), isopropyl alcohol (IPA) and Li_2CO_3 (E. Merck Darmstadt) as a pore-former were mechanically mixed in a supersonic mixer. The carbon and PTFE loadings were maintained at a fixed content of 5 and 2.5 mg cm^{-2}, respectively, and compounded with Li_2CO_3 under IPA. The amount of pore-former was varied in the order: 0, 3, 5, 7 and 10 mg cm^{-2}. The viscous mixture was rolled on to the wet-proofed carbon cloth and then dried at 80 °C for 1 h. Next, the diffusion backing (i.e. diffusion layer deposited on carbon cloth) was treated with 1 M H_2SO_4 and then washed several times with distilled water. In this step, Li_2CO_3 is removed by dissolving the salt in aqueous sulfuric acid. Again, after drying at 80 °C for 1 h, the sample was sintered in air at 350 °C. We call this second process, i.e. pore-former and heat treatment, as pore-forming treatment. Finally, a thin catalyst layer was prepared by means of a hot coating method. That is, 0.4 mg cm^{-2} Pt, 20 wt.% on Vulcan XC-72R (Electrochem Inc.), 0.75 mg cm^{-2} Nafion solution (5 wt.%, Aldrich) and IPA were mixed and brushed on to the diffusion layer which is fixed on a hot plate at 45 °C using a silicon blade. Therefore, the catalyst layer in the electrode was PTFE-free. For effective contact between the catalyst and the polymer electrolyte,

Nafion solution of 2 mg cm^{-2} was sprayed again on the catalyst layer and the latter was dried in an oven at 80 °C. Nafion®115 membranes were pretreated with H_2O_2 and H_2SO_4 to remove organic and mineral impurities, respectively. Next, the membranes were rinsed several times with hot distilled water. MEAs were fabricated by hot pressing at 120 °C and 3 t for 3 min.

2.2. Investigation of morphological characteristics

The morphological characteristics of the diffusion layer were measured using scanning electron microscopy (SEM, H-6010, Hitachi Co.) and mercury-intrusion porosimetry. SEM provided the real image of surface structure of the diffusion layer at each preparation step. Information on the internal structure of diffusion layer was obtained using a pore-size analyzer (Autopore III 9420, Micromeritics Inc.), which measures the amount of mercury penetration as a function of the applied pressure.

2.3. Cell operation and electrochemical analyses

A single PEMFC was operated at a cell temperature of 75 °C, and the humidification temperatures of the anode and cathode gases were maintained at 10 and 5 °C higher than the cell temperature, respectively. MEAs with a rather small active area of 1 cm^2 were used. Thus, it can be assumed that gas utilization is constant throughout the whole reaction area. The feed flow rates of the anode and cathode gases were kept in the range of 200–250 ml min^{-1} for optimum cell performance. All single-cell operations were performed without external pressurization. Current density versus cell voltage curves of single-cells were obtained with a system dc electronic load (6060B, Hewlett-Packard) and a personal computer programmed for data acquisition. A potentiostat/galvanostat (model 273, EG&G) equipped with a lock-in amplifier (model 5210, EG&G) was used for ac impedance analysis. The reference and counter electrode were connected to the anode, and the working electrode was linked to the cathode. Impedance spectroscopy was measured at various dc potentials between 0.9 and 0.4 V. The frequency was varied from 100 kHz to 100 mHz, and the ac signal amplitude was 10 mV rms.

3. Results and discussion

3.1. Morphological change of diffusion layer

The pore-size distribution in the diffusion layer is shown in Fig. 2. It can be seen (Fig. 2(a)) that the diffusion layer has two distinctive changes of pore-size distribution before (type A) and after (type B and C) pore-forming treatment. To identify these structural changes in different pore-size ranges, the pores in the diffusion layer are divided according to size into five classes and attention is focused on three size

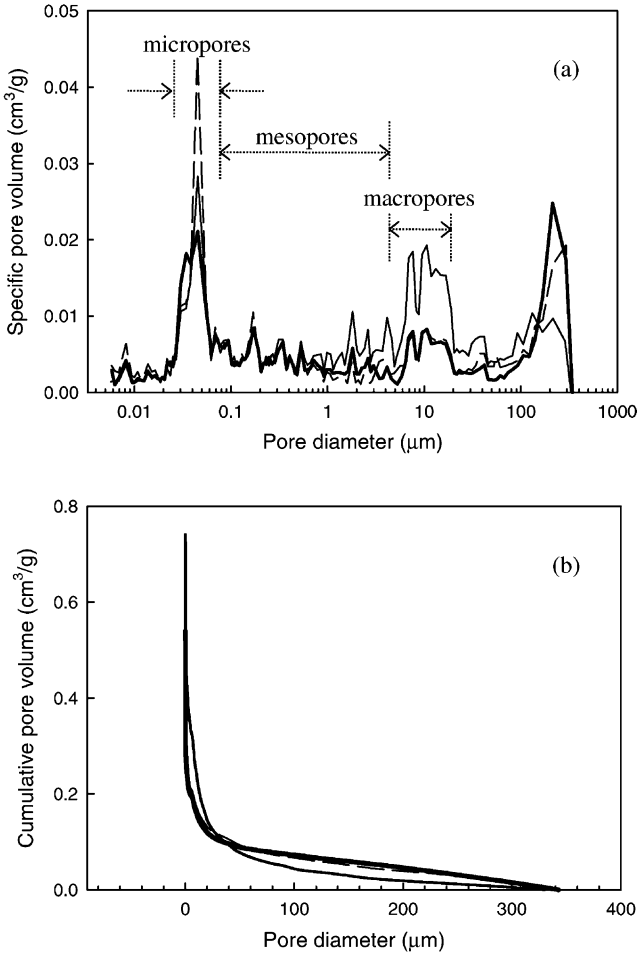

Fig. 2. (a) Specific and (b) cumulative pore-size distribution of diffusion layer obtained from mercury-intrusion porosimetry measurements: (▬) type A, (– – –) type B, (—) type C electrodes.

ranges, namely: macropores (pore diameter from 5 to 20 μm) and micropores (pore diameter from 0.03 to 0.06 μm), which are two pore ranges that show conspicuous variation in the specific pore volume, and mesopores (the intermediate range between 0.06 and 5 μm). The definition of each pore range is based on the porosimetry data on the diffusion layers used only in this study and hence, it is entirely different from the general criteria for classifying 'micro', 'meso' and 'macro' pores. The size of pores larger than about 100 μm stems from the fissures on the surface of the diffusion layer. It is found that the volume of the micropores increases after heat treatment at 350 °C (type B) and that the macropore volume increases after the pore-former has been dissolved out through acid-treatment (type C). By contrast, the mesopore volume remains uninfluenced, without significant difference, in spite of the pore-forming treatment. The effect of heat treatment on the diffusion layer has been demonstrated in many studies. As shown by the results of Cheng et al. [15], at a temperature of 350 °C, PTFE melts and transforms into a fiber phase along with dispersant removal. Thus, it is seen that the change in the micropore

Table 1
Classification of electrodes and morphological characteristics of diffusion layer

Electrode	Pore-forming treatment[a]		Pore diameter (μm)				
	PF	HT	Total porosity (%) 0.006–300	Local porosity (%)			
				0.006–0.03	0.03–0.06	0.06–5	5–20	20–300
Type A	No	No	49.6	4.43	7.45	19.72	7.13	10.85
Type B	No	Yes	51.7	5.56	8.60	18.48	7.19	11.88
Type C	Yes	Yes	55.2	3.34	6.07	20.56	14.38	10.85

[a] PF: pore-former treatment (140 wt.%), HT: heat treatment (at 350 °C).

volume is due to melting and re-dispersion of PTFE in the interior of the diffusion layer by the heat treatment. In addition, when pore-former and heat treatment are employed together in diffusion layer preparation, the micropore volume decreases during the macropore generation process. Apparently, the range of pore-size is broadly distributed between 0.006 and 300 μm, but small pores with diameters less than 20 μm occupy about 80% of the total pore volume (Fig. 2(b) and Table 1). To estimate the extent of variation in pore-size distribution, the variation in the porosity of the diffusion layer is calculated according to the criteria defined above and is summarized in Table 1. Here, total porosity refers to the ratio of total volume of the void fraction to the geometric volume of the diffusion layer, while local porosity is defined as the ratio of the volume of pores in a certain size range to the geometric volume of the diffusion layer. Note that the variation of total porosity, in spite of the pore-forming treatment, is not larger than predicted.

The microstructure of the diffusion layer at each preparation step was verified by scanning electron micrographs. Micrographs of the top-view of the diffusion layer are shown in Fig. 3. The pore structure formed by addition of pore-former is dependent on the nature of the material chosen as a pore-former. Li_2CO_3 used in the experiments is composed of rod-like particles with average length and mean diameter of about 50 and 5 μm, respectively. Comparison of Fig. 3(c) and (e) with Fig. 3(a) demonstrates that macropores with sizes of 5–10 μm are generated on the surface of the diffusion layer after acid-treatment for melting the pore-former in the diffusion layer. The structural change of the porous surface observed at a smaller scale, cf., Fig. 3(b, d and f), can obviously be seen after the specimen was heat-treated at 350 °C.

3.2. H_2/O_2 and H_2/air single-cell performance test

The significance of macropores in the diffusion layer was examined through performance tests of a H_2/O_2 single-cell for which the pore-former content was varied from 0 to 200 wt.% carbon loading. Performance curves obtained in the H_2/O_2 regime (Fig. 4) show that the drop in cell voltage in the high current density region decreases as the amount of pore-former increases. The deviation from a linear drop in cell voltage with current density is minimized at a 140 wt.% pore-former loading, and then increases at contents of 200 wt.%. This suggests that there exists an optimum amount of pore-former, in other words, there is an appropriate macropore volume of the diffusion layer which is desirable for cell performance enhancement. For the H_2/O_2 system, water flooding is known to be the main limiting factor which restricts the improvement of performance at high current densities. The higher the current density, the faster the water generation rate. Unless reactants are supplied sufficiently to the reaction sites, the reactant concentration becomes exhausted and brings about a significant drop-in performance. From Fig. 5, we can verify that the optimum loading of pore-former enhances the electrode performance mostly in the high current density region (over 600 mA cm^{-2} in the present study), where mass-transport limitation dominates cell performance.

An explanation of our experimental results can be derived by examining water condensation phenomena in the porous media. Consider a single pore within the diffusion layer. If its diameter is smaller than the critical pore-size (r_c), water condensation will occur before the vapor pressure reaches saturation pressure at a given temperature. Thus, small pores will be filled with liquid water earlier, within the size range governed by the Kelvin equation (below several tens of nanometers), than large pores. The smaller the pore-size and porosity, the larger is the overpotential due to the mass-transport limitation. The modeling results of Bevers et al. [9] showed that larger pore-size and higher porosity of catalyst layer and diffusion layer are beneficial in reducing the fall-off in performance at high current densities. Likewise, it is thought that such an internal situation in the porous electrode will be maintained until the pressure difference across the liquid and vapor water interface becomes lower than the capillary pressure determined by the well-known Young–Laplace equation. According to the calculations of Bernardi and Verbrugge [4], pores less than about 1 μm in size can sustain a liquid-phase pressure which is approximately 1 atm greater than the vapor-phase pressure. Consequently, macropores produced by the pore-former are capable of reducing the mass-transport limitation due to water flooding since they can provide gas diffusion paths toward the catalytic region until the micropores and the smaller pores are completely closed by water droplets. This interpretation does not mean, however, the macroporous diffusion layer,

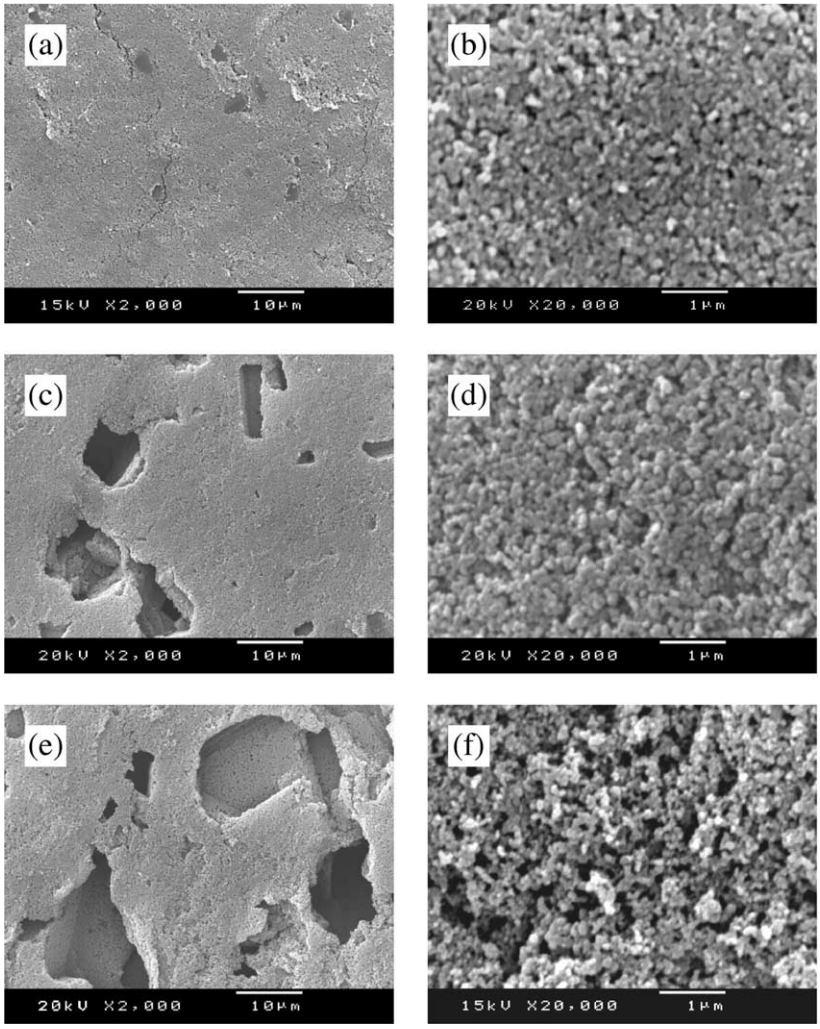

Fig. 3. Scanning electron micrographs of surface of diffusion layer at each preparation step. (a and b) Before acid-treatment for pore-former removal; (c and d) after acid-treatment; and (e and f) after heat treatment at 350 °C.

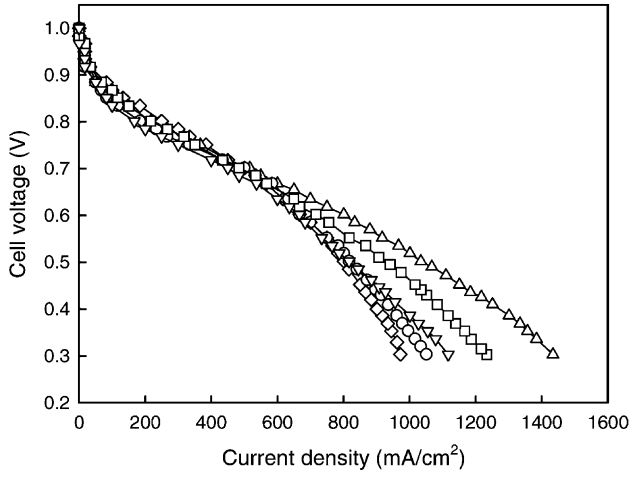

Fig. 4. Influence of pore-former content in diffusion layer on cell performance of H_2/O_2 single-cells: (◇) 0 mg cm^{-2}, (○) 3 mg cm^{-2}, (□) 5 mg cm^{-2}, (△) 7 mg cm^{-2}, and (▽) 10 mg cm^{-2} pore-former loading. In all cases, 5 mg cm^{-2} carbon loading in diffusion layer and 0.4 mg Pt cm^{-2} in catalyst layer.

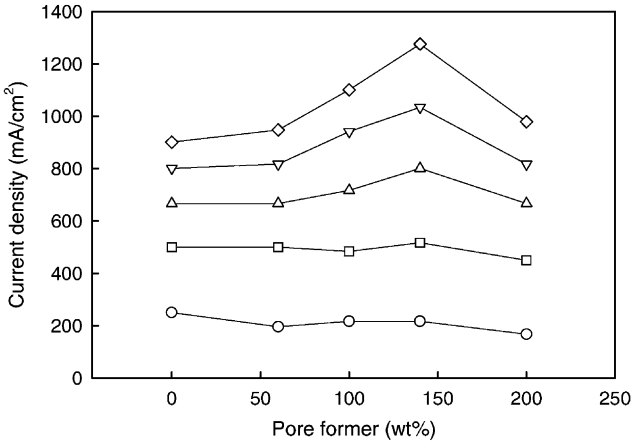

Fig. 5. Current density as function of pore-former content in diffusion layer of H_2/O_2 single-cell at different voltages: (○) 0.8 V, (□) 0.7 V, (△) 0.6 V, (▽) 0.5 V, (◇) and 0.4 V.

which consists of macropores only, is effective in ameliorating the water flooding problem. The study of Wilson et al. [6] showed that serious water flooding occurs in macroporous carbon paper with a mean pore-size of 30 μm. In addition, if the macropore volume is too large, the electric conductivity of the electrode is decreased. Therefore, the performance improvement in the present study can be attributed to the effect of the microstructure of the diffusion layer where macropores and micropores co-exist in an appropriate ratio. Most of all, it is important to realize that the pore-size distribution, i.e. the ratio of macropore volume and micropore volume, of diffusion layer is the more influential parameter, compared with total porosity.

The results of performance tests of an air-operated cell is shown in Fig. 6. These show that the electrode with a pore-former-treated diffusion layer also exhibits a better performance under a H_2/air regime. One prominent feature is that the improvement is extended to the lower current density region as well as at the high current densities. When using air oxidant, because nitrogen gas occupies a substantial portion of reaction zone, the effective reaction area is reduced relative to that in the case of a pure oxygen supply. In other words, because of the low oxidant concentration (decreased by a factor of five) at the reaction sites, the oxygen reduction reaction becomes the rate-limiting step of the overall fuel cell reaction and results in a drastic drop in cell voltage even in the low current density region. Furthermore, if the effect of water flooding is included, the mass-transfer condition within the porous electrode is exacerbated.

3.3. Impedance analysis of H_2/O_2 single-cell operation

The impedance spectra of a H_2/O_2 single-cell measured at voltages of 0.7 and 0.4 V are presented in Fig. 7. All points in the frequency arc in both impedance spectra overlap each other along the slope of about 45° and thus the semicircle size is determined by the size of the low-frequency arc. At a cell voltage of 0.7 V, the diameter of the semicircle, which corresponds to the polarization resistance (R_p), decreases with increase in the amount of pore-former; the minimal value is at 7 mg cm^{-2} (140 wt.%) of pore-former loading. The largest impedance loop is observed at a pore-former content of 10 mg cm^{-2} (200 wt.%); that is, the polarization resistance of the electrode with a diffusion layer in which excessive amount of pore-former is used is larger than that of an electrode prepared without pore-former. The polarization resistance is a combination of charge-transfer resistance and diffusion resistance. As the current density increases, the diffusion resistance becomes more dominant than the charge-transfer resistance. That is, the polarization resistance becomes mass-transfer controlled. Therefore, as the current density increases, the size of the impedance loop in general shows a pattern in that it decreases in the low current density region through the reduced effect of charge-transfer resistance and then increases in the high current density region through the enlarged effect of diffusion resistance [16]. The important fact that can be obtained from Fig. 7(a) is that the diffusion layer structure, modified by the pore-former, is effective to reduce polarization resistance even at low current densities.

The variation of polarization resistance and double-layer capacitance (C_{dl}) as a function of pore-former content in the diffusion layer is shown in Fig. 8. At a cell voltage of 0.4 V, the polarization resistance is relatively high compared with

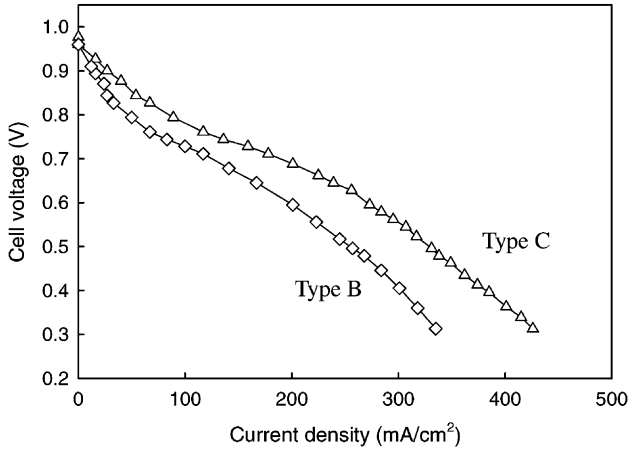

Fig. 6. Comparison of performance curves of H_2/air single-cell operated under atmospheric pressure condition: (◇) 0 mg cm^{-2}, (△) 7 mg cm^{-2} pore-former loading, 5 mg cm^{-2} carbon loading in diffusion layer and 0.4 mg Pt cm^{-2} in catalyst layer.

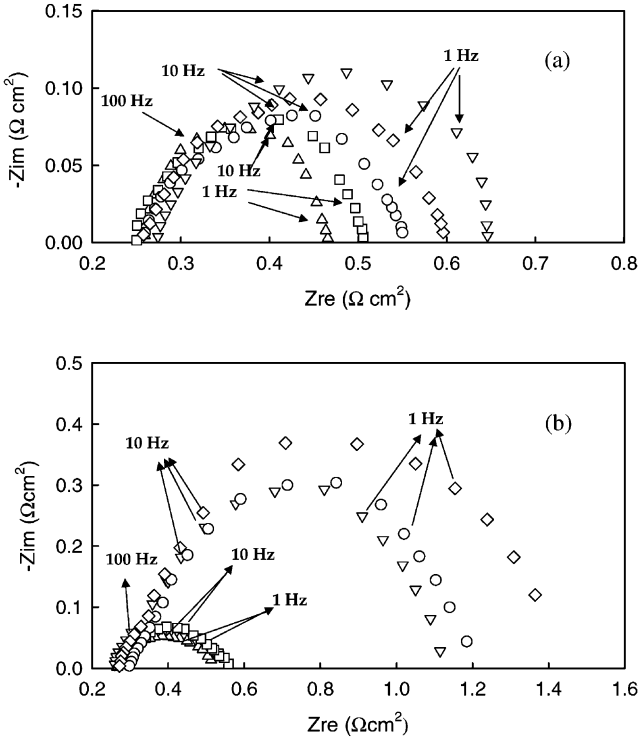

Fig. 7. Impedance plots as function of pore-former content in diffusion layer of H_2/O_2 single-cell at voltage of (a) 0.7 V and (b) 0.4 V. (◇) 0 mg cm^{-2}, (○)3 mg cm^{-2}, (□) 5 mg cm^{-2}, (△) 7 mg cm^{-2}, and (▽)10 mg cm^{-2}.

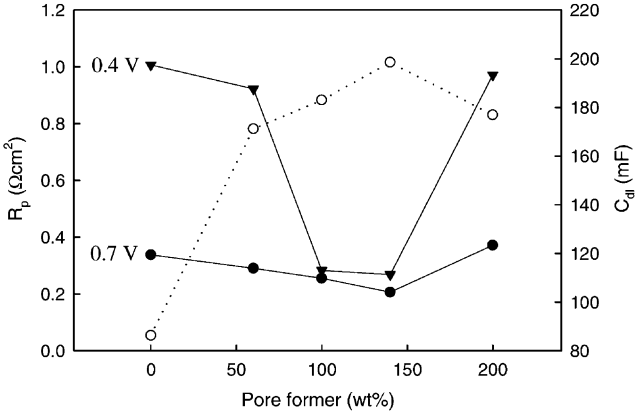

Fig. 8. Dependence of polarization resistance, R_p, at (●) 0.7 V and (▼) 0.4 V and double-layer capacity, C_{dl}, (○) at 0.7 V, on pore-former content in diffusion layer of H_2/O_2 single-cell.

that for the 0.7 V condition. It can be seen, however, that the polarization resistance at 0.4 V is reduced to approximately as low as the R_p level at 0.7 V when the optimum dose of pore-former is applied. Such variation of R_p indicates that the diffusion resistance, which is responsible for the increase in polarization resistance at high current densities, is decreased and hence the mass-transport characteristics within the electrode are improved. It is also seen that the double-layer capacitance which is proportional to the active reaction area, increases with increase in pore-former content in the diffusion layer. This indicates that the morphology of the diffusion layer has a significant influence on the double-layer capacitance and appears to be related with the catalyst layer characteristics. When a catalyst slurry is applied directly on to the diffusion layer, as in the present experiment, the slurry fills up the pores on the surface of the diffusion layer and then forms a thin catalytic layer on the diffusion layer. Therefore, the surface morphology of the diffusion layer can determine the catalyst layer structure and affect the effective reaction area throughout the catalyst layer. Now, the results of Fig. 7(a) can be explained. The amount of pore-former is directly related to the pore structure of the diffusion layer, and diffusion layer structure affects the catalytic features of the catalyst layer. As the result, pore-former treatment of the diffusion layer can make important contributions to the decrease of polarization resistance in the charge-transfer controlled region. Similar observation has been made by Giorgi et al. [10] with varying amounts of PTFE in the diffusion layer.

4. Conclusions

The microstructure of the diffusion layer is modified by employing a pore-former, Li_2CO_3, and heat treatment at 350 °C. An examination is made of the effect of the pore-size distribution and the porosity of the diffusion layer on the cell performance characteristics of H_2/O_2 and H_2/air single PEMFCs. As a result, it is verified that the pore-size distribution is a more important structural parameter in affecting the cell performance characteristics than the total porosity. The macropores in the diffusion layer are thought to prevent water flooding of electrodes and, hence, the performance loss can be reduced by enhancement of the mass-transport process. When this electrode structure is applied to the H_2/air system, the cell performance is improved over the whole current density region. Thus, in order to minimize the effect of the mass-transport limitation, it is desirable to tailor the morphology of diffusion layer with control of pore-size distribution.

Acknowledgements

The authors are grateful to Kyoung-Hwan Choi of Samsung Advanced Institute of Technology and Sung-Jin An of Clean Energy Technologies Inc. for helpful comments and discussions. Thanks are also due to the Korea Research Institute of Chemical Technology for performing mercury porosimetry measurements. This work was supported by Korea Research Foundation Grant. (KRF-2001-005-E00030).

References

[1] H.H. Voss, D.P. Wilkinson, P.O. Pickup, M.C. Johnson, V. Basura, Electrochim. Acta 40 (1995) 321–328.
[2] T.V. Nguyen, Electrochem. Soc. 143 (1996) L103–L105.
[3] D.L. Wood III, J.S. Yi, T.V. Nguyen, Electrochim. Acta 43 (1998) 3795–3809.
[4] D.M. Bernardi, M.W. Verbrugge, J. Electrochem. Soc. 139 (1992) 2477–2491.
[5] Y.W. Rho, O.A. Velev, S. Srinivasan, Y.T. Kho, J. Electrochem. Soc. 141 (l994) 2084–2096.
[6] M.S. Wilson, J.A. Valerio, S. Gottesfeld, Electrochim. Acta 40 (1995) 355–363.
[7] R. Mosdale, S. Srinivasan, Electrochim. Acta 40 (1995) 413–421.
[8] V.A. Paganin, E.A. Ticianelli, E.R. Gonzalez, J. Appl. Electrochem. 26 (1996) 297–304.
[9] D. Bevers, M. Wohr, K. Yasuda, K. Oguro, J. Appl. Electrochem. 27 (1997) 1254–1264.
[10] L. Giorgi, E. Antolini, A. Pozio, E. Passalacqua, Electrochim. Acta 43 (1998) 3675–3680.
[11] L.R. Jordan, A.K. Shukla, T. Behrsing, N.R. Avery, B.C. Muddle, M. Forsyth, J. Power Sources 86 (2000) 250–254.
[12] E. Passalacqua, G. Squadrito, F. Lufrano, A. Patti, L. Giorgi, J. Appl. Electrochem. 31 (2001) 449–454.
[13] A. Fischer, J. Jindra, H. Wendt, J. Appl. Electrochem. 28 (1998) 277–282.
[14] E. Passalacqua, I. Gatto, F. Lufrano, A. Patti, G. Squadrito, in: Proceedings of the 2000 Fuel Cell Seminar, Portland, 2000, pp. 118–121.
[15] X. Cheng, B. Yi, M. Han, J. Zhang, Y. Qiao, J. Yu, J. Power Sources 79 (1999) 75–81.
[16] T.E. Springer, T.A. Zawodzinski, M.S. Wilson, S. Gottesfeld, J. Electrochem. Soc. 143 (1996) 587–599.